15. Mc Neill AJ, Fioretti PM, El-Said EM, Salustri A, Forster T, Roelandt JRTC. Enhanced sensitivity for detection of coronary artery disease by addition of atropine to dobutamine stress echocardiography. *Am J Cardiol* 1992;70:41–46.
16. Elhendy A, Geleijnse ML, Roelandt JRTC, et al. Evaluation by quantitative ^{99m}Tc-MIBI SPECT and echocardiography of myocardial perfusion and wall motion abnormalities in patients with dobutamine-induced ST-segment elevation. *Am J Cardiol* 1995;76:441–448.
17. Arnese M, Cornel JH, Salustri A, et al. Prediction of improvement of regional left ventricular function after surgical revascularization: a comparison of low-dose dobutamine echocardiography with ^{201}Tl SPECT. *Circulation* 1995;91:2748–2752.
18. Baptista J, Arnese M, Roelandt JRTC, et al. Quantitative coronary angiography in the estimation of the functional significance of coronary stenosis: correlation with dobutamine-atropine stress test. *J Am Coll Cardiol* 1994;23:1434–1439.
19. Ruffolo RR. The pharmacology of dobutamine. *Am J Med Sci* 1987;294:244–248.
20. Warltier DC, Zyvoloski M, Gross GJ, Hardman HF, Brooks HL. Redistribution of myocardial blood flow distal to a dynamic coronary arterial stenosis by sympathomimetic amines: comparison of dopamine, dobutamine and isoproterenol. *Am J Cardiol* 1981;48:269–279.
21. Abraham RD, Freedman SB, Dunn RF, et al. Prediction of multivessel coronary artery disease and prognosis early after acute myocardial infarction by exercise electrocardiography and ^{201}Tl myocardial perfusion scanning. *Am J Cardiol* 1986;58:423–427.
22. Allman KC, Berry J, Sucharski LA, et al. Determination of extent and location of coronary artery disease in patients without prior myocardial infarction by ^{201}Tl tomography with pharmacologic stress. *J Nucl Med* 1992;33:2074–2079.
23. Armstrong WF, O'Donnell J, Rayan T, Feigenbaum H. Effect of prior myocardial infarction and extent and location of coronary artery disease on accuracy of exercise echocardiography. *J Am Coll Cardiol* 1987;10:531–538.
24. Sutton JM, Topol EJ. Significance of a negative exercise thallium test in the presence of a critical residual stenosis after thrombolysis for acute myocardial infarction. *Circulation* 1991;83:1278–1286.
25. Oosterhuis WP, Niemeyer MG, Kuijper AF, et al. Evaluation of the incremental diagnostic value and impact on patient treatment of thallium scintigraphy. *J Nucl Med* 1992;33:1732–1734.

Pre- and Post-Therapy Thallium-201 and Technetium-99m-Sestamibi SPECT in Nasopharyngeal Carcinoma

Lale Kostakoglu, Uğur Uysal, Enis Özyar, Nazenin Elahi, Mutlu Hayran, Dilek Uzal, Figen B. Demirkazik, Ayşe Kars, Ömer Uğur, Lale Atahan and Coşkun F. Bekdik

Departments of Nuclear Medicine, Radiation Oncology, Radiology, Medical Oncology and Cancer Epidemiology, Hacettepe University Medical Center, Ankara, Turkey

We prospectively studied the diagnostic potential of ^{201}Tl and ^{99m}Tc-sestamibi (MIBI) SPECT for evaluating the extent of primary disease and differentiating residual/recurrent disease from post-therapy changes in patients with nasopharyngeal carcinoma (NPC). **Methods:** Fifty patients (20 initial presentation, 30 post-therapy evaluation) underwent ^{201}Tl and MIBI imaging. The findings were correlated with CT/MRI results. Tumor-to-background ratios were obtained. Biopsy confirmation (14 patients) and/or 6–12 mo clinical follow-up data (16 patients) were available in the post-therapy group. **Results:** All primary disease sites were accurately detected by both imaging studies in the pretherapy group. However, MIBI-SPECT was superior to ^{201}Tl SPECT ($p = 0.0057$) in detecting regional metastases (sensitivities of 95% versus 68%). In the post-therapy group, MIBI and ^{201}Tl imaging were true-positive in 14 of 16 patients with proven residual/recurrent. In 17 patients who had no evidence of residual/recurrent tumor, CT/MRI was false-positive in 13 when MIBI and ^{201}Tl imaging were true-negative in 10 and false positive in 3. MIBI, ^{201}Tl and CT/MRI had sensitivities of 87.5%, 87.5%, 100%, specificities of 82.4%, 76.5%, 23.5% and accuracies of 85%, 82%, 61%, respectively. Tumor-to-background ratios were ≤1.5 in all false-positive cases except one. **Conclusion:** MIBI-SPECT proves more accurate than ^{201}Tl SPECT in detecting regional metastases at initial presentation. MIBI and ^{201}Tl imaging have higher specificity and accuracy than CT/MRI and MIBI-SPECT is slightly more specific than ^{201}Tl SPECT in differentiating residual/recurrent disease from post-therapy changes in patients with NPC.

Key Words: nasopharyngeal carcinoma; thallium-201; technetium-99m-sestamibi; residual disease; SPECT

J Nucl Med 1996; 37:1956–1962

Nasopharyngeal carcinoma (NPC) is recognized as a potentially curable disease using combined modality treatments, despite the low survival rates reported thus far (*1*). Early diagnosis, treatment and follow-up of NPC are important to improve survival rates. Proper assessment of primary and metastatic NPC requires clinical/fiberoptic examination followed by biopsy when necessary, CT/MRI examination of the nasopharynx and thorax and bone scintigraphy. CT/MRI is the test of choice for accurate locoregional staging at initial presentation. Moreover, subclinical tumor extension to parapharyngeal and retropharyngeal spaces is detected only by these modalities (*2–4*). After therapy, the clinical situation is complicated by post-therapy changes in the anatomic planes that constitute a diagnostic dilemma in the majority of patients. It is important to avoid false-positive results since they may lead clinicians to perform unnecessary treatment options.

Although imaging technology has improved, a gold standard imaging modality is needed to differentiate viable tumor from post-therapy changes. Postgadolinium-enhanced MRI has been reported to be superior to CT in differentiating necrosis from active tumors, but its false-positive rate for residual/recurrent disease is still unacceptably high (*5,6*). There is also increasing evidence that PET may allow differentiation between inflammatory changes and viable tumor (*7,8*). More recently, ^{11}C-methionine has been used to assess treatment response to radiotherapy in head and neck cancer (*9,10*). However, its availability and cost are still major limiting factors. There has been growing interest in functional imaging using ^{201}Tl and MIBI. These agents provide useful tumor imaging information to differentiate physiologic from pathologic uptake in patients with various cancers (*11–14*). Unfortunately, there is scarce data on scintigraphic evaluation of the extent of primary NPC, its regional or distant metastases, as well as in monitoring the response to treatment and distinguishing residual/recurrent tumor from post-therapy changes (*15,16*). We thought that clinical application of these tumor imaging agents might further

Received Dec. 28, 1995; revision accepted Apr. 10, 1996.
For correspondence or reprints contact: Lale Kostakoglu, MD, Hacettepe Üniversity Tïp Fakültesi, Nükleer Tïp Anabilim Daï, Sïhhiye 06100 Ankara, Turkey.

refine NPC staging and increase the accuracy in detecting residual disease after treatment. In this study, we evaluated the contribution of ^{201}Tl and MIBI scintigraphy to evaluating the extent of primary disease as compared with radiographic modalities and to differentiating residual/recurrent disease from post-therapy changes as compared with CT/MRI findings in patients with NPC.

MATERIALS AND METHODS

We prospectively studied 50 patients with histologically-proven NPC, who presented either for initial workup before therapy (20 patients) or follow-up after therapy (30 patients) during 15 mo between September 1994 and December 1995. There were 38 men and 12 women with a mean age of 44 yr (range 13–72 yr). Thirty-eight patients had undifferentiated carcinoma (WHO type III), 12 had squamous-cell carcinoma or nonkeratinizing epidermoid carcinoma (WHO type I and II) (*17*). There were 41 patients at Stage IV, five at Stage III and four at Stage II. All patients had contemporaneous CT/MRI studies and bone scintigraphy and results were correlated with the findings on ^{201}Tl and MIBI scintigraphy.

Pretherapy Group

Twenty consecutive patients were included in the study before radiotherapy and chemotherapy. The patients underwent imaging and radiographic studies 7 to 21 days after biopsy of the primary lesion. Nineteen patients had CT, and one patient had MRI studies. CT or MRI was used as a gold standard with which the results of the scintigraphic studies were compared.

Post-therapy Group

Thirty patients were studied after therapy. Histopathologic (14 patients) and/or 6–12-mo clinical follow-up data (16 patients) were used as the gold standard against which the results of the scintigraphic and radiographic studies were compared. Fifteen patients had MRI and 15 had CT studies. The interval between imaging studies and completion of therapy ranged from 3 to 20 mo (mean 8 mo). All patients had received 60–70 Gy to the nasopharynx and 46–70 Gy to the cervical and supraclavicular lymph nodes. Twenty-one patients had also received cisplatin-based chemotherapy consisting of cisplatin and 5-fluorouracil or cisplatin, bleomycin and methotrexate. Fourteen patients had biopsy confirmation performed within 7 to 15 days of scintigraphic and radiographic studies. Nasopharyngeal biopsy was performed in 11 patients, fine-needle aspiration in one and excisional biopsy in two for doubtful cervical lymph node metastases. In those patients whose histopathology revealed no evidence of viable tumor, we obtained 6–12-mo follow-up data and confirmed the results by stable CT/MRI findings and normal endoscopic examination in order to avoid possible false-negative biopsy results that could stem from sampling errors. For 16 patients, we did not have histopathologic confirmation as there was no appreciable mass to biopsy in the nasopharynx on endoscopic examination in nine patients, there were distant metastases in five, rendering biopsy unnecessary, and two patients were considered to have a recurrent tumor by CT/MRI criteria and clinical evaluation (Table 2, Patients 4 and 16). In these 16 patients, 6–12-mo follow-up data, repeated CT/MRI and endoscopic examinations were available.

Imaging Studies

A dual-head ADAC Genesys camera interfaced with an ADAC Pegasys SP10 computer system was used for image acquisition. A low-energy, general-purpose collimator was used for ^{201}Tl, and a low-energy, high-resolution collimator was used for MIBI imaging. The time interval between ^{201}Tl and MIBI imaging ranged from 3 hr to 5 days. Thallium-201 scintigraphy was performed before MIBI imaging in all patients. All patients were pretreated with potassium perchlorate (6 mg/kg) to suppress physiological uptake of ^{201}Tl and MIBI in the salivary glands. All patients underwent whole-body scintigraphy and SPECT of the head and neck 30 min after the administration of 111 MBq ^{201}Tl and 555 MBq MIBI. SPECT was performed in a circular step-and-shoot mode, at 360° for sixty-four 30-sec views using a matrix size of 64 × 64 and a zoom-factor of 1.85. SPECT projections were reconstructed using a filtered backprojection technique with a Butterworth filter, a cutoff frequency of 0.5, an order of 10 for ^{201}Tl SPECT and a Gaussian filter, a cutoff frequency of 0.5 and an order of 20 for MIBI SPECT. After attenuation correction, images were displayed in coronal, sagittal and transverse slices. Tumor-to-background ratios were obtained using ROIs drawn in consecutive coronal slices that contained the entire tumor volume. For MIBI imaging, physiologic uptake in the head and neck was noted in the pituitary glands, nasal and oral cavity, pharyngeal recesses, bilaterally, maxillary sinuses, parotids, palatine, submandibular and sublingual salivary glands. Any uptake other than physiologic uptake was considered positive for residual/recurrent or metastatic disease. The scintigraphic studies were interpreted by two nuclear physicians and a consensus was reached regarding the findings.

CT scans were obtained using a Philips Tomoscan SR 7000 scanner, 3–5-mm sections and using IV contrast. MRI was performed using Philips Gyroscan TII in multiple planes with both T1- and T2-weighted pulse sequences using IV Gd-DTPA for evaluating primary disease in the nasopharynx and its extension to the regional lymph nodes and adjacent tissues. At least one coronal and sagittal T1-weighted and one axial T2-weighted sequence was included in the MRI examination. Slice thickness ranged from 3 to 5 mm. The images were interpreted as either suggesting residual/recurrent mass or no residual/recurrent mass by an experienced radiologist.

Statistical analysis was performed using SPSS for Windows, version 5.01. The sensitivity, specificity and accuracy of scintigraphic and radiographic modalities were calculated by taking the biopsy data in 14 patients and clinical follow-up data in 16 patients as a gold standard.

RESULTS

The ^{201}Tl and MIBI uptake in the salivary glands was not affected by stimulation of the discharge mechanism of the salivary glands with potassium perchlorate ingestion in all patients.

Pretherapy Group

Nasopharynx. The results of ^{201}Tl and MIBI imaging and CT/MRI data are summarized in Table 1. There were no false-negative studies for the primary disease located in the nasopharynx for both scintigraphic studies (Figs. 1A, B). The size of the tumors detected in the nasopharynx ranged between 3 and 7 cm. Due to the necrotic component in the core of the large tumors, radiotracer uptake was heterogeneous, and the tumor-to-background ratios were relatively lower than those with no necrotic component on CT/MRI. The mean tumor-to-background ratio in the nasopharynx was 3.76 ± 1.34 (range 2.4 to 6.4) for MIBI-SPECT and 2.35 ± 0.67 (range 1.3 to 3.52) for ^{201}Tl SPECT (Table 1). There was a statistically significant difference between the ratios obtained from ^{201}Tl and MIBI scintigraphies ($p < 0.0001$; Wilcoxon test).

Lymph Nodes. Cervical lymph nodes were involved to various degrees in all but four patients. Among 16 patients with cervical lymph node involvement there were 19 sites, 18 of which were detected by MIBI-SPECT (95%). One metastatic lymph node could not be detected because of the overlying physiologic uptake in the adjacent parotid gland. The size of the

TABLE 1
Tumor/Background Ratios in Nasopharynx and Metastatic Sites in the Pretherapy Group

Nasopharynx			Cervical lymph nodes and distant metastases					
Patient no.	^{201}Tl	MIBI	Patient no.	^{201}Tl	MIBI	CT/MRI	Site	Size (cm)*
1	1.30	1.71	1	1.80	2.20	+†	CLN	5
2	1.86	2.44		−FN	2.50	+	CLN	5
3	2.30	3.51	2	1.90	1.54	+	CLN	5
4	2.43	2.80	3	1.80	1.48	+	CLN	2
5	1.50	2.40		1.81	1.50	+	CLN	1
6	1.90	2.70	4	2.10	5.30	+	CLN	10
7	1.91	3.00	5	−FN	1.40	+	CLN	2
8	1.62	2.54	6	1.47	1.35	+	CLN	8
9	2.10	4.31	7	2.32	4.00	+	CLN	10
10	3.70	6.40		2.00	2.10	+	CLN	3
11	2.10	2.90	8	−FN	1.35	+	CLN	2
12	3.31	5.00	9	2.94	7.00	+	CLN	8
13	2.85	5.06	10	—	—	—		
14	1.70	2.41	11	—	—	—		
15	2.10	3.00	12	−FN	−FN	+	CLN	2.5
16	2.00	4.00	13	2.20	2.90	+	CLN	2
17	2.81	5.00	14	1.85	2.80	+	CLN	3
18	2.80	5.30	15	−FN	2.05	+	CLN	3
19	2.61	6.05	16	1.95	1.94	+	SCL	3
20	3.00	3.65	17	3.13	2.95	+	CLN	5
			18	−FN	1.45	+	CLN	2.5
			19	—	—	—		
			20	—	—	—		
Mean±s.d.	2.35 ± 0.67	3.76 ± 1.34	Mean±s.d.	2.09 ± 0.47	2.59 ± 1.75			

*Greatest diameter.
†Lymph node metastasis detected by CT.
CLN = cervical lymph node; SCL = supraclavicular lymph node; FN = false-negative.

minimal detectable lymph node was 1 cm for both MIBI and ^{201}Tl SPECT. The detectability of lymph node involvement was not dependent on lesion size for either imaging study (Table 1). Of the 19 metastatic lymph nodes, ^{201}Tl SPECT was false-negative in six. The size of these lymph nodes ranged from 1.5 to 5 cm (Figs. 2A, B). The results for CT/MRI, MIBI and ^{201}Tl scintigraphy were statistically different from one another in detecting primary disease ($p = 0.0057$; Cochran Q-test). Further analysis using McNemar's test revealed that MIBI findings were not different from those of the gold standard (CT/MRI) ($p = 1.0$), whereas the results for ^{201}Tl were significantly different from those of the gold standard ($p = 0.03$)

The mean tumor-to-background ratios for the disease in the region of cervical lymph nodes were 2.59 ± 1.75 (range: 1.35–5.3) and 2.09 ± 0.47 (range: 1.47–3.13) for MIBI and ^{201}Tl SPECT, respectively (Table 1). There was a statistically significant difference between the ratios obtained from ^{201}Tl and MIBI scintigraphies ($p < 0.0001$; Wilcoxon test). Overall sensitivity for MIBI and ^{201}Tl imaging was 97% and 85%, respectively, for detecting primary disease and its regional metastases (Table 3). Specificity could not be determined due to inadequate number of true-negative sites.

Post-Therapy Group

The results of ^{201}Tl, MIBI, CT/MRI and biopsy data are summarized in Table 2. Table 3 shows the percentage sensitivity, specificity and accuracy of ^{201}Tl, MIBI imaging compared with CT/MRI. In 30 patients, 33 sites were evaluated for the presence or absence of residual/recurrent or metastatic disease after therapy. Based on histologic confirmation in 14 patients and 6- to 12-mo clinical follow-up in 16, there was recurrent/residual or metastatic disease in 16 sites (7 nasopharynx, 5 bony metastases, 4 cervical lymph nodes). Of the 16 sites, both ^{201}Tl and MIBI imaging were true positive in the corresponding 14 sites (87.5%), while CT/MRI was true positive in all 16 (100%) (Table 3). The minimal detectable lesion was 1.6 cm for both MIBI and ^{201}Tl SPECT. Both scintigraphic methods failed to detect metastatic sites in the bones (vertebra, pelvis), but bone scintigraphy successfully detected these sites (Fig. 3). On the other hand, both ^{201}Tl and MIBI scintigraphy were true positive in the other three patients who had bony metastases (Table 2; Patients 3, 10, 29).

There was no evidence of recurrent/residual disease in 17 sites as proven by biopsy (eight patients) and/or clinical follow-up (nine patients). Biopsy data revealed chronic inflammation and/or necrotic tissue in all specimens negative for tumors. Keeping sampling errors in mind, we confirmed the negative results with the patients' 6- to 12-mo clinical follow-up data. MIBI was true-negative in 14 (82%) sites when CT/MRI was true-negative in only four (23.5%) sites (Table 3). CT/MRI was false-positive in 13 (76%) sites when MIBI was also false-positive in the corresponding 3 sites (18%). Thallium-201 imaging was true-negative in 13 sites that correspond to the same sites as those negative for tumor on MIBI imaging and false-positive in four patients, two of whom also had false-positive MIBI and CT/MRI. The other two false-positive patients on ^{201}Tl imaging were true-negative on MIBI imaging (Table 2, Patients 11 and 18) when one was true-negative and the other was false-positive on CT/MRI (Figs. 4A, B).

The mean tumor-to-background ratio was 2.85 ± 1.35 (range 1.50 to 5.30) for MIBI and 1.75 ± 0.49 (range 1.2 to 3.51) for ^{201}Tl imaging for all true-positive cases (Table 2). There was a

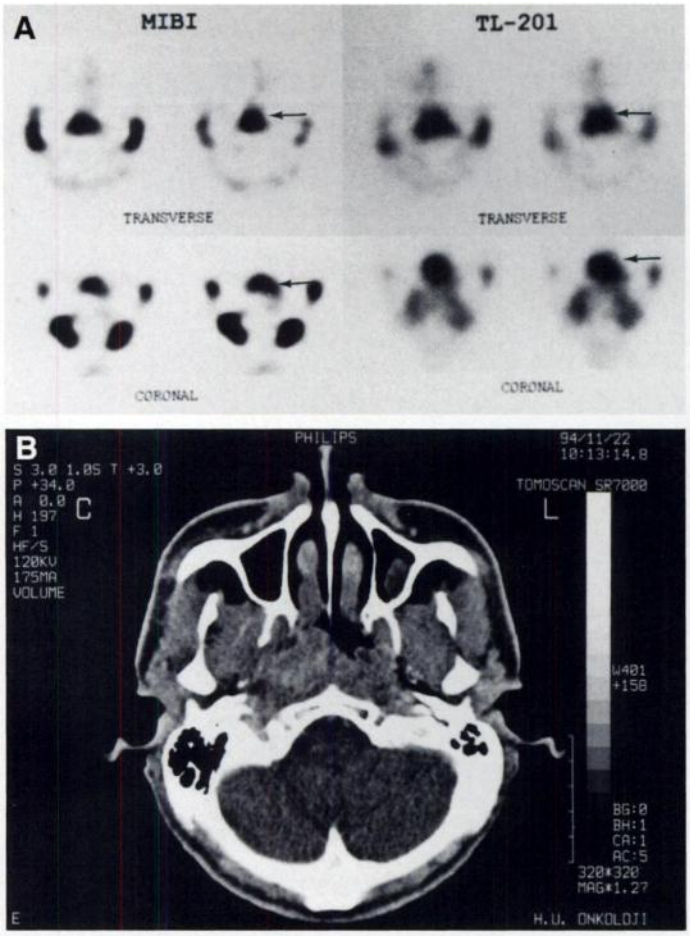

FIGURE 1. (A) Transverse (upper panels) and coronal slices (lower panels) of MIBI and ^{201}Tl SPECT studies, respectively, reveal intense radiotracer uptake in the region of nasopharynx (arrows) consistent with a malignant process. (B) CT study of the nasopharynx demonstrates a mass obliterating the pharyngeal recesses, bilaterally, and extending anteriorly towards the nasal cavity consistent with NPC.

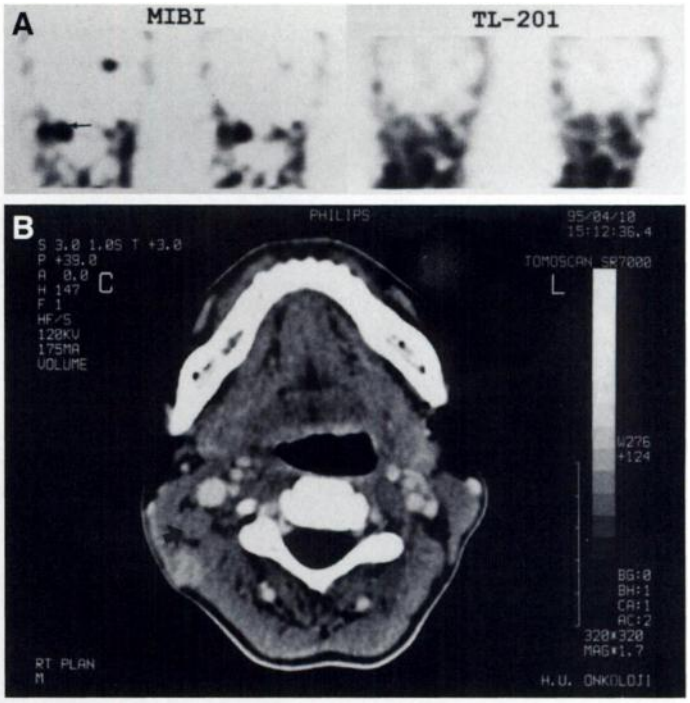

FIGURE 2. (A) Coronal slices of MIBI SPECT head and neck study demonstrate an area of increased focal uptake in the right superior cervical region consistent with lymph node metastasis, whereas coronal slices of ^{201}Tl SPECT of the corresponding region do not show any discernible focus of abnormal radiotracer accumulation. Additionally, the other focus of radiotracer uptake superiorly in the left is consistent with the secretion of MIBI through the ventricles; right ventricle is not symmetrically visualized because of the patient's slightly tilted position. (B) CT study of the nasopharynx shows an enlarged lymph node (arrow) in the right upper cervical region consistent with lymph node metastasis.

statistically significant difference between the ratios obtained from ^{201}Tl and MIBI scintigraphies ($p < 0.0001$; Wilcoxon test).

Neither the results for ^{201}Tl nor those for MIBI were statistically different from one another for predicting residual/recurrent or metastatic NPC ($p = 0.65$; Cochran Q-test). Using the Kappa test, the concordance between the findings on the gold standard (biopsy and/or 6–12-mo follow-up data) and those on MIBI and ^{201}Tl imaging were 69.7% (s.e. = 12.4%) and 63.7% (s.e. = 13.29%), respectively. The mean tumor-to-background ratios were 1.59 ± 0.17 and 1.47 ± 0.22 for false-positive MIBI and ^{201}Tl imaging, respectively.

DISCUSSION

Imaging is an integral part of clinical staging and treatment planning in NPC patients (*1,2,18*). At initial presentation, CT or MRI is the test of choice for outlining the size of the tumor and its extension to adjacent tissues (*1,19*). After therapy, PET appears promising in differentiating post-therapy changes from residual/recurrent disease in head and neck cancers, but its availability is still a major limitation (*9,10*). On the other hand, much more practical scintigraphic techniques are in demand in oncology, such as ^{201}Tl and MIBI imaging. Because of the rarity of NPC, neither of these agents has been studied extensively for detecting primary tumors or differentiating post-therapy changes from viable tumor.

Pretherapy Group

We found an overall sensitivity of 97% for MIBI and 85% for ^{201}Tl imaging in detecting primary tumor and regional lymph nodes (Table 3). In contrast to our findings, Kao et al. (*15*) reported a sensitivity of 70% for MIBI imaging in patients with NPC. The lower sensitivity rates obtained in this previous study could be due to the differences in patient populations and to different acquisition protocols and camera sensitivities. We used a dual-headed camera with a relatively longer acquisition time to increase sensitivity and a zoom factor to have adequate resolution. In our study, ^{201}Tl detected the primary tumor in all patients, while it failed to detect 32% of the regional metastatic lymph nodes (Fig. 2A). On the other hand, MIBI-SPECT detected 95% of the metastatic lymph nodes and missed one that was adjacent to the parotid gland. The differences in the metabolic rate of glucose utilization, enzyme function and ATPase pump could account for different distribution patterns in the primary site and metastases. Since ^{201}Tl accumulation is considered a reflection of ATPase activity and energy consumption, tumors with lower metabolic rates may not accumulate ^{201}Tl (*13*). In a previous study, ^{201}Tl uptake was reported to be an indicator of viable tumor cells with faster DNA synthesis (*20*). Similarly in our study, the proliferation rate of the primary tumor might be higher than that of the metastatic sites. In rapidly proliferating cells, the activity of the ATPase pump and mitochondrial oxidative capacity will increase both MIBI and ^{201}Tl uptake and retention. However, in cells of lower metabolism, although ATPase activity slows down, membrane potentials and mitochondrial activity will be spared allowing adequate MIBI uptake.

TABLE 2
Tumor/Background Ratios in the Post-therapy Group

Site	^{201}Tl	Ratio	MIBI	Ratio	CT/MRI	Biopsy	Res/rec dis*
1. SCL	TP	1.25	TP	1.55	+TP	+	+
2. NPX	TN	—	TN	—	+FP	−	−
3. Bone	TP	1.61	TP	1.82	+TP	NP	+
4. NPX	TP	2.00	TP	3.82	+TP	NP	+
5. NPX	FP	1.45	FP	1.55	+FP	−	−
6. NPX	TN	—	FP	1.80	+FP	−	−
7. SCL	TP	1.85	TP	2.10	+TP	+	+
8. NPX	TN	—	TN	—	+FP	−	−
9. NPX	FP	1.25	FP	1.47	+FP	NP	−
10. CLN Bone	TP	1.72	TP	3.41	+TP	NP	+
	TP	1.71	TP	1.74	+TP	NP	+
11. NPX	FP	1.80	TN	—	+FP	−	−
12. NPX	TN	—	TN	—	−TN	NP	−
13. NPX	TP	1.43	TP	2.00	+TP	+	+
14. NPX	TP	1.70	TP	4.92	+TP	+	+
15. NPX	TP	1.92	TP	5.30	+TP	+	+
16. NPX	TP	1.65	TP	2.70	+TP	+	+
18. NPX	FP	1.50	TN	—	−TN	NP	−
19. NPX	TN	—	TN	—	−TN	NP	−
20. NPX	TN	—	TN	—	−TN	NP	−
21. NPX	TN	—	TN	—	+FP	NP	−
22. NPX	TN	—	TN	—	+FP	NP	−
23. NPX	TN	—	TN	—	+FP	NP	−
24. NPX Bone	TP	1.73	TP	3.15	+TP	NP	+
	TN	—	TN	—	+FP	NP	−
26. NPX	TN	—	TN	—	+FP	−	−
27. NPX	TN	—	TN	—	+FP	−	−
28. NPX	TN	—	TN	—	+FP	−	−
29. NPX Bone	TP	3.51	TP	4.90	+TP	NP	+
	TP	1.94	TP	1.54	+TP	NP	+
30. Bone	FN	—	FN	—	+TP	NP	+
Mean ± s.d.		1.75 ± 0.49		2.85 ± 1.35			

*Clinical decision for residual or recurrent disease by biopsy and/or clinical follow-up.
SCL = supraclavicular lymph node; NPX = nasopharynx; NP = not performed; CLN = cervical lymph node; FP = false-positive; TN = true-negative; TP = true-positive; FN = false-negative.

TABLE 3
Statistical Analysis in Nasopharynx and Cervical Lymph Nodes

	Pretherapy group				Post-therapy group		
	^{201}Tl	^{201}Tl	MIBI	MIBI	^{201}Tl	MIBI	CT/MRI
	NPX	LN	NPX	LN			
TP	20	13	20	18	14	14	16
TN	0	4	0	4	13	14	4
FP	0	0	0	0	4	3	13
FN	0	6	0	1	2	2	0
Sensitivity (%)	100	68.4	100	94.7	87.5	87.5	100
Specificity*† (%)					76.5	82.4	23.5
Accuracy (%)	100	85	100	95.6	81.8	84.8	60.7
PPV	100	100	100	100	77.7	82.4	55.2
NPV	†	40	†	80	86.7	87.5	†

*There were no true-negative cases to determine specificity.
†There were not enough true-negative cases to determine specificity.
NPX = nasopharynx; LN = lymph nodes; TP = true-positive; TN = true-negative; FP = false-positive; FN = false-negative; PPV = positive predictive value; NPV = negative predictive value.

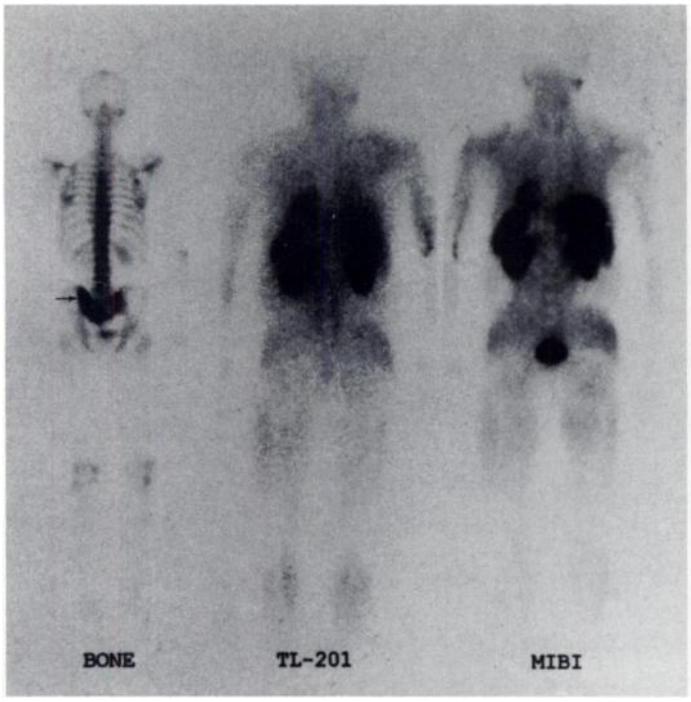

FIGURE 3. Posterior whole-body bone image depicts an area of intense increased radiotracer uptake in the left sacroiliac joint extending towards posterior iliac crest where the patient experiences excruciating pain (arrow). This focus was consistent with bony metastatic disease, but posterior whole-body images of both MIBI and ^{201}Tl studies were false-negative by not revealing any focus of increased radiotracer uptake in the corresponding region.

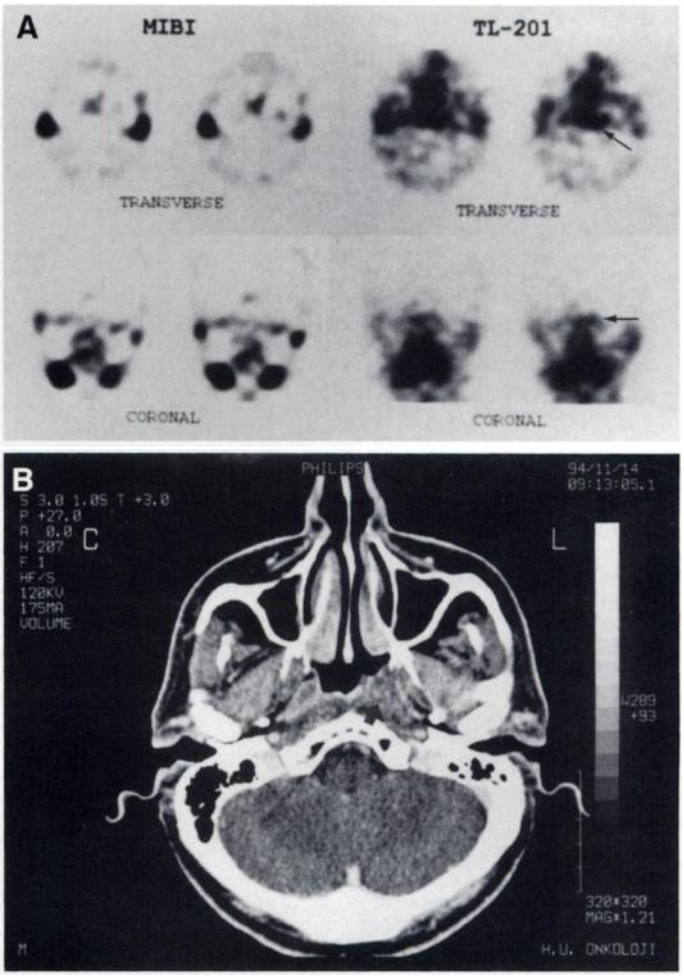

FIGURE 4. (A) Transverse slices (arrows, upper panel) and coronal slices (arrows, lower panel) of MIBI SPECT head and neck study, do not demonstrate any area of abnormal radiotracer uptake in the nasopharynx. However, the ^{201}Tl SPECT study shows a focus of increased radiotracer uptake in the nasopharynx extending towards the right pharyngeal nasopharynx (arrows). (B) CT study of the nasopharynx performed 4 mo after completion of therapy shows a residual mass in the nasopharynx (arrow) interpreted as residual/recurrent NPC, but biopsy of the corresponding region revealed chronic inflammatory changes with no evidence of residual carcinoma. Ten-month clinical follow-up data confirmed biopsy findings rendering ^{201}Tl and CT results false-positive.

Post-Therapy Group

In the clinical setting, intracavitary brachytherapy and/or small-field external irradiation is added to the therapy protocol when there is a radiographically or histologically persistent tumor (*23*). Therefore, a specific functional imaging modality is most needed when radiographic modalities depict a mass indistinguishable from the residual/recurrent tumor. In this study, we found higher specificity and accuracy for both scintigraphic methods as compared with radiographic modalities. MIBI imaging allowed greater specificity and accuracy than ^{201}Tl imaging. Togawa et al. (*16*) suggested that ^{201}Tl imaging should be used to monitor response to therapy in NPC, but they did not comparatively study MIBI imaging to determine the better imaging agent. Furthermore, their series did not have an adequate number of patients (9 patients) to determine firm conclusions (*16*).

Tumor-to-background ratios were $\leq$1.5 in all false-positive cases, except for two patients (Table 2; Patients 6 and 11). This finding was in accordance with most post-therapy benign conditions having uptake ratios below 1.5 (*13*). Since biopsy results of these false-positive sites revealed chronic inflammation and dense vasculature, high blood flow in the inflammatory tissue might influence uptake of radiotracers. Alternatively, the accumulation of ^{201}Tl or MIBI might occur passively due to altered permeability of injured cell membranes in irreversible cell death, since three of five false-positive scans were obtained after 3 to 4 mo of radiotherapy, a period during which the effects of radiotherapy might continue. There were three mismatched false-positive ^{201}Tl and MIBI studies (Table 2; Patients 6, 11, 18). Two of three patients with false-positive ^{201}Tl and true-negative MIBI histologically had ongoing nasopharyngeal infections. Due to the increased proliferation rate, ^{201}Tl imaging may tend to show false-positive in infections. The other patient (Table 2; Patient 6) evaluated 3 mo after radiotherapy underwent MIBI-SPECT 10 days before ^{201}Tl SPECT, a period during which inflammatory changes could regress and render false-negative studies as true-negative. False-negative results obtained for bone metastases may be ascribed to the lower extraction fraction of radiotracers by the skeleton.

CONCLUSION

MIBI imaging was found to be more sensitive in detecting lymph nodes and more specific and accurate than ^{201}Tl and CT/MRI in differentiating post-therapy changes from residual/recurrent disease. Therefore, MIBI-SPECT may be incorporated into the work-up of patients with NPC at initial presentation to obtain baseline studies and after therapy to elucidate the nature of persistent masses. However, false-negative results for the disease sites adjacent to the parotid/salivary glands and in the bones should be taken into consideration. Nonetheless, currently MIBI cannot obviate the need of repeated histologic confirmation to avoid false-negative results caused by sampling errors. Therefore, there is clearly a need for a further trial with more patients and longer follow-up periods to determine the influence of MIBI on patient management.

REFERENCES

1. Altun M, Fandi A, Dupuis O, et al. Undifferentiated nasopharyngeal cancer (UCNT). Current diagnostic and therapeutic aspects. *Int J Radiat Oncol Biol Phys* 1995;32: 859–877.
2. Celai E, Olmi P, Chiavacci A, et al. Computed tomography in NPC. Part I:T stage conversion with CT staging. Part II: impact on survival. *Int J Radiat Oncol Biol Phys* 1990;19:1171–1182.
3. Sham JST, Choy D. Prognostic value of paranasopharyngeal extension of nasopharyngeal carcinoma on local control and short-term survival. *Head Neck* 1991;13: 298–310.
4. Teo P, Shiu W, Leung SF, Lee WY. Prognostic factors in nasopharyngeal carcinoma investigated by computer tomography–an analysis of 659 patients. *Radiother Oncol* 1992;23:79–93.
5. Franc J, Vanel D, Schwaab G, Eschwege F, Micheau C. Interet de l'imagerie par resonnance magnetique dans le bilan initial et la surveillance des carcinomes indifferencies de typr nasopharynge (UCNT). *Rev Im Med* 1991;3:181–185.
6. Marano I, Brunetti A, Covella M, et al. Magnetic resonance in the diagnosis and follow up of soft tissue sarcomas. *Radiology Med* 1992;84:15–21.
7. Rege S, Maas A, Chaiken L, et al. Use of PET with fluorodeoxyglucose in patients with extracranial head and neck cancers. *Cancer* 1994;73:3047–3058.
8. Zeitouni AG, Yamamato YL, Black M, Gjedde A. Functional imaging of head and neck tumors using PET. *J of Otolaryngology* 1994;23:77–80.
9. Lindholm P, Leskinen-Kallio, Grenman R, et al. Evaluation of response to radiotherapy in head and neck cancer by PET and [^{11}C]methionine. *Int J Radiat Oncol Phy* 1995;32:787–794.
10. Leskinen-Kallio S, Lindholm P, Lopela M, et al. Imaging of head and neck tumors with PET and [^{11}C]methionine. *Int J Radiation Oncology Biol Phy* 1995;30:1195–1199.
11. Ramannah L, Waxman AD, Binney G, Waxman S, Mirra J, Rosen G. Tl-201 scintigraphy in bone sarcoma: comparison with Ga-67 and Tc-99m MDP in the evaluation of chemotherapeutic response. *J Nucl Med* 1990;31:567–571.
12. Abdel-Dayem H, Scott AM, Macapinlac HA, El-Gazzar AH, Larson SM. Role of Tl-201-chloride and Tc-99m-sestamibi in tumor imaging. In: Freeman LM, ed. *Nuclear medicine annual*. New York: Raven Press; 1994:181–234.
13. Kostakoglu L, Panicek D, Divgi CR, et al. Comparative study with Tl-201-chloride, MRI, angiography in patients with soft-tissue sarcomas following treatment. *Eur J Nucl Med* 1995;22:1232–1237.
14. Schwartz RB, Cavalho PA, Alexander E III, Loeffler JS, Folkerth R, Holman BL. Radiation necrosis versus high-grade recurrent glioma: differentiation by using dual-isotope SPECT with Tl-201 and Tc-99m-HMPAO. *Am J Neuroradiol* 1991;12: 1187–1192.
15. Kao CH, Wang SJ, Lin WY, Hsu CY, Liao SQ, Yeh SH. Detection of nasopharyngeal carcinoma using Tc-99m-methoxyisobutylisonitrile SPECT. *Nucl Med Commun* 1993; 14:41–46.
16. Togawa T, Yui N, Kinoshita F, Shimada F, Omura K, Takemiya S. Visualization of nasopharyngeal carcinoma with Tl-201-chloride and three-head rotating gamma camera SPECT system. *Ann Nucl Med* 1993;7:105–113.
17. World Health Organization. Histological typing of upper respiratory tract tumors. In: *International histological classification of tumors*, no. 19. Geneva, Switzerland: World Health Organization; 1978:32–33.
18. Mendenhall WM, Million RR, Maneuso AA, Stringer SP. Nasopharynx. In: Millon RR, Cassisi NJ, eds. *Management of head and neck cancer. A multidisciplinary approach*, 2nd ed. Philadelphia, PA: J.B. Lippincott; 1994.
19. Yu Z, Xu G, Huang Y, Hu YH, Su XG, Gu XZ. Value of computed tomography in staging the primary lesion (T-staging) of nasopharyngeal carcinoma: an analysis of 54 patients with special reference to the parapharyngeal space. *Int J Radiat Oncol Biol Phys* 1985;11:2143–2147.
20. Venuta S, Ferraiuolo R, Morrone G, et al. The uptake of Tl-201 in normal and transformed thyroid cell lines. *J Nucl Med Allied Sci* 1979;23:163–166.
21. Backus M, Piwnica-Worms D, Hockett D, et al. Microprobe analysis of Tc-99m-MIBI in heart cells: calculation of mitochondrial membrane potential. *Am J Physiol* 1993;265:178–187.
22. Hall ZW. *An introduction to molecular neurobiology*. Sunderland, MA: Sinauer; 1992: 33–178.
23. Taifu L. Trends in the clinical management of nasopharyngeal carcinoma. *Int J Radiat Oncol Biol Phys* 1992;23:469–471.

Prognostic Value of Thyroglobulin after Thyroidectomy before Ablative Radioiodine Therapy in Thyroid Cancer

Frank Grünwald, Christian Menzel, Rolf Fimmers, Paul O. Zamora and Hans J. Biersack

Department of Nuclear Medicine, and Institute for Medical Statistics, University of Bonn, Bonn, Germany

Serum thyroglobulin (Tg) is a suitable marker for differentiated thyroid carcinoma after total thyroid ablation by surgery and ^{131}I therapy. Before the first ^{131}I treatment, Tg is not a reliable tumor marker since it can also originate from remnant tissue. It was hypothesized that the ratio of serum Tg to ^{131}I uptake in the thyroid bed could be used to correct Tg values for variations in remnant tissue. **Methods:** The hypothesis was evaluated in 111 patients with differentiated thyroid cancer (38 follicular/73 papillary). Tg and ^{131}I uptake in the thyroid bed were measured before the first ^{131}I therapy. The ratio of Tg to ^{131}I uptake was determined in four groups: Group A, tumor free (n = 81); Group B, lymph node metastases (n = 11); Group C, distant metastases (n = 11); Group D, later recurrence [during a mean follow-up of 56 mo; (n = 8)]. Wilcoxon two-sample test was performed to determine statistical significance between Group A and Groups B-D. **Results:** Significant differences in the Tg/^{131}I uptake ratios (median) between Group A (1.0 ng/ml/%) and Groups B (3.3 ng/ml/%), C (20.2 ng/ml/%) and D (3.3 ng/ml/%) were observed ($p < 0.01$). In tumor-free patients (Group A), there was no value higher than 5.7 ng/ml/%. Therefore, a higher ratio, observed in 14 of the 30 remaining patients, was indicative of metastases or later recurrence. **Conclusion:** The ratio of serum Tg to ^{131}I uptake in the thyroid bed might be used as a prognostic marker for thyroid cancer before implementing ablation with ^{131}I.

Received Jan. 11, 1996; revision accepted Apr. 5, 1996.

For correspondence or reprints contact: F. Grünwald, MD, Department of Nuclear Medicine, University of Bonn, Sigmund Freud Strasse 25, 53127 Bonn, Germany.

Key Words: thyroglobulin; prognosis; thyroid cancer; radioiodine therapy

J Nucl Med 1996; 37:1962–1964

Small amounts of serum thyroglobulin (Tg) can be found in the serum of most healthy people, but it can be elevated in several benign thyroid diseases (*1,2*) and in thyroid cancer (*3–10*). Since Tg is a normal tissue component, it can only be reliably used as a "tumor marker" after total thyroid ablation, such as after thyroidectomy and ablative ^{131}I therapy. In these cases, serum Tg is a very reliable marker for the local recurrence of thyroid cancer, lymph node metastases and distant-site metastases. Serum Tg has the advantage of high sensitivity (>90%) in detecting recurrence and/or metastases and can be used under TSH-suppressive thyroxine therapy (although the sensitivity of serum Tg also depends on TSH).

Scintigraphy with ^{131}I is used as a generalized "marker" for thyroid tissue as a result of its uptake and subsequent incorporation into tissue Tg, whether it be in the normal thyroid remnant or in thyroid cancers. Whole-body scintigraphy with ^{131}I is commonly used to detect the recurrence of thyroid carcinoma and/or metastatic lesions. The procedure requires thyroid hormone withdrawal to induce hypothyroidism and maximize uptake of ^{131}I and its subsequent incorporation into Tg. In some cases, whole-body scintigraphy fails to detect